Available online at www.sciencedirect.com
SCIENCE DIRECT®
Journal of Nuclear Materials 325 (2004) 53–60
journal of nuclear materials
www.elsevier.com/locate/jnucmat

Recrystallization and precipitation behavior of low-activation V–Cr–Ti alloys after cold rolling

N.J. Heo [a,*], T. Nagasaka [b], T. Muroga [b]

[a] Department of Fusion Science, School of Mathematical and Physical Science, The Graduate University for Advanced Studies, Toki-shi, Gifu 509-5292, Japan
[b] National Institute for Fusion Science, Toki-shi, Gifu 509-5292, Japan

Received 18 August 2002; accepted 30 October 2003

Abstract

Recrystallization and precipitation behavior after cold working were investigated for three V–4Cr–4Ti alloys, NIFS-HEAT-1, NIFS-HEAT-2 and US 832665, which contain different levels of impurities. The decrease in hardness and the initiation of recrystallization against test temperature do not depend on the oxygen level. However, the rate of grain growth decreased with the increase in the impurity levels. Bimodal distribution of the precipitates was observed after annealing at 1273 K. The large precipitates were Ti-rich precipitates, and the small ones were composed mainly of Ti, C and O (Ti–C–O precipitates). The impurities were dissolved from Ti–C–O precipitates above 1273 K, and the level of impurities in the matrix increased and resulted in the increase in the hardness. Based on the results, the annealing temperature for V–4Cr–4Ti alloys is recommended not to exceed 1273 K for the purpose of maintaining good mechanical properties such as tensile and impact properties.

1. Introduction

Vanadium alloys have been identified as one of the promising candidate structural materials for fusion first wall/blanket applications, due to their low induced radioactivity, good resistance to neutron radiation damage and good elevated-temperature strength [1–4]. Based on the previous studies, V–4Cr–4Ti alloy was selected as a leading candidate [4].

Recently high-purity 30 and 166 kg V–4Cr–4Ti ingots (NIFS-HEAT-1 and 2) were fabricated by NIFS (National Institute for Fusion Science) [5,6]. The oxygen content of NIFS-HEATs are almost half that of large heat of V–4Cr–4Ti produced by a US-DOE (Department of Energy) program [7,8]. It is well known that impurities such as oxygen, nitrogen and carbon have various effects on properties of vanadium alloys [9–11]. It is assumed that the various properties in NIFS-HEATs are different from other V–4Cr–4Ti alloys including the US-DOE heat, because of the low impurity level.

In vanadium alloys, the precipitates induced by impurities and their distribution have a great effect on various properties [12]. Thus, it is necessary to investigate the precipitation behavior under the fabrication processes including thermal and mechanical treatments.

The purpose of this study is to clarify the behavior of recrystallization and precipitation by annealing after cold working, for three kinds of V–4Cr–4Ti alloys, NIFS-HEAT-1, 2 and US 832665, with different levels of oxygen. The results will be discussed in relation to the redistribution of impurities.

2. Experimental procedure

Table 1 shows chemical composition of the V–Cr–Ti alloys used in this study. US 832665 is a V–4Cr–4Ti

* Corresponding author. Tel.: +81-572 58 2317/2319; fax: +81-572 58 2676.
E-mail address: heonj@nifs.ac.jp (N.J. Heo).

0022-3115/$ - see front matter © 2003 Elsevier B.V. All rights reserved.
doi:10.1016/j.jnucmat.2003.10.012

Table 1
Chemical composition of V–4Cr–4Ti alloys used (mass ppm for C, N, O concentration)

	Cr (wt%)	Ti (wt%)	C	N	O
NIFS-HEAT-1	4.12	4.13	56	103	181
NIFS-HEAT-2	3.9	3.89	62	84	158
US 832665	3.8	3.9	80	85	310

large ingot (500 kg melt) fabricated by a US-DOE program [7]. The major difference in the composition of the three alloys is the level of oxygen. The thermomechanical treatment after melting for the NIFS-HEATs was the hot forging at 1423 K and the hot or cold rolling. They were then cut into 10 mm after hot working. The US 832665 was a 3.8 mm thick plate, which was hot-extruded at 1423 K and warm-rolled at 673 K. All plates, NIFS-HEATs and US 832665, were cold-rolled to 90% thickness reduction into about 1 and 0.4 mm thick sheets, respectively.

After mechanical polishing and electro-polishing, the specimens were sandwitched with tantalum sheets and wrapped with zirconium getter foils, followed by annealing at the range of 473–1373 K for 1 h in a vacuum ($<10^{-3}$ Pa). After annealing, micro-Vickers hardness tests were conducted in the condition of load of 500 gf and loading time of 30 s. Microstructural observations were also carried out using optical microscope, SEM (scanning electron microscope) and TEM (transmission electron microscope).

3. Results

Fig. 1 shows the hardness changes of each specimen as a function of the annealing temperature. Fig. 1 shows no significant difference in the hardness curves for the three alloys, in spite of the difference in the oxygen content. The hardness of NIFS-HEAT-2 was lower than that of other two samples at most temperatures.

For all alloys, hardness started to drop at 873 K. Hardness for NIFS-HEAT-1, 2 and US 832665 reached to a minimum value at 1223, 1173 and 1273 K, respectively. The minimum hardness temperature increases with increasing the impurity level. Hardening was observed in all specimens by annealing above the minimum hardness temperature. The hardness decrease of NIFS-HEAT-1 annealed at 1073 K was larger than that of the US 832665.

Fig. 2 shows the development of optical microstructure with annealing temperature from as-rolled condition to 1373 K. Microstructural change was not found to 873 K in the optical microscopic scale. All the specimens were entirely recrystallized at 1173 K, but they

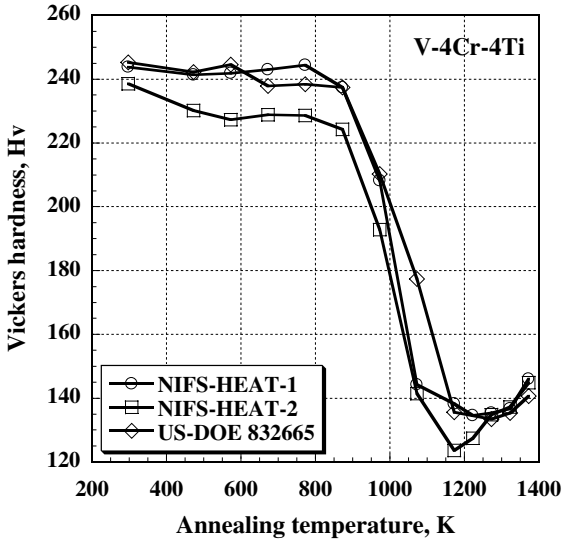

Fig. 1. Hardness change of the three alloys as a function of the annealing temperature. The annealing was carried out for an hour.

showed elongated grain structures parallel to the cold-rolling direction. Table 2 shows the grain size and the aspect ratio measured in rolling plane for three annealing temperatures and two directions. When annealed at 1173 K, The aspect ratio for NIFS-HEAT-1, NIFS-HEAT-2 and US 832665 was about 0.58, 0.55 and 0.75, respectively. Isotropic recrystallized grains formed by annealing at 1273 K. Annealing at 1373 K in all the specimens resulted in grain coarsening.

Fig. 3 shows SEM image of NIFS-HEAT-1 annealed at 873 K for an hour. The microstructural observation revealed that recrystallization already started at 873 K in all specimens. In this case, recrystallization took place partially with the size of recrystallized grains smaller than 10 μm. Fig. 3 means that recrystallization starts at the same temperature independent of interstitial impurity levels.

Fig. 4 shows the change of the grain size with annealing temperature. At 1173 K there was no great difference in grain size among the three alloys. However, in NIFS-HEATs grain size significantly increased with annealing temperature. On the other hand, the change in the grain size with annealing temperature is small for US-DOE 832665. Fig. 4 suggests that the rate of grain growth decreases with the increase of the impurity levels.

Fig. 5 indicates the precipitate distribution in the transverse plane of the three alloys annealed at 1273 K for an hour. In NIFS-HEATs, the precipitates were aligned along the rolling direction. On the other hand, the precipitates in US-DOE 832665 were uniformly distributed in the matrix.

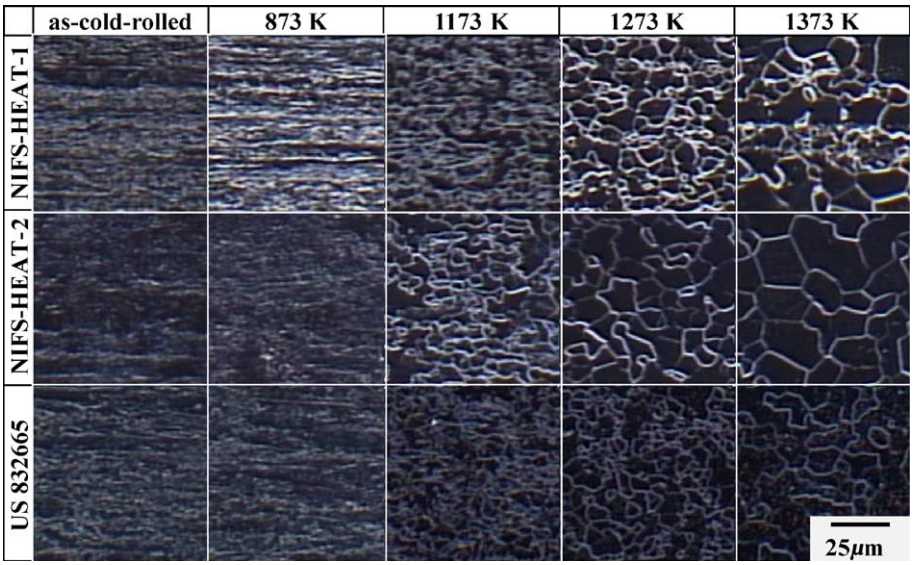

Fig. 2. Development of the grain structures with annealing temperature after rolling. The annealing was carried out for an hour.

Table 2
Size and aspect ratio of grains of the specimens annealed at various temperatures

Direction	1173 K		1273 K		1373 K	
	Grain size (μm)	Aspect ratio	Grain size (μm)	Aspect ratio	Grain size (μm)	Aspect ratio
NIFS-HEAT-1						
Rolling	11.92	0.58	11.55	0.82	23.81	0.91
Transverse	6.94		9.45		21.74	
NIFS-HEAT-2						
Rolling	13.32	0.55	16.26	0.84	29.06	0.91
Transverse	7.39		13.63		26.41	
US-DOE832665						
Rolling	9.58	0.75	10.32	0.81	12.48	0.95
Transverse	7.19		8.39		11.84	

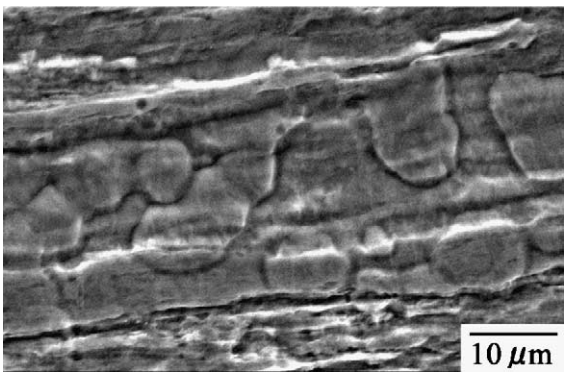

Fig. 3. SEM image of NIFS-HEAT-1 annealed at 873 K for an hour. Recrystallization occurred with the grain size below 10 μm.

Fig. 6 is SEM images on the surface of V–4Cr–4Ti alloys annealed at 1273 and 1373 K. No precipitates were observed on the grain boundaries when annealed at 1273 K, but fine precipitates were formed on the grain boundaries at 1373 K.

Fig. 7 shows the result of compositional analysis with SEM–EDS (energy dispersive X-ray spectroscopy) on the grain boundary including precipitates, for NIFS-HEAT-1 annealed at 1373 K. As shown in Fig. 7, carbon content is higher at the precipitates. The concentration of chromium, titanium, oxygen and nitrogen was however almost homogeneous.

Fig. 8 is the bright field images of TEM obtained from the NIFS-HEAT-1 annealed at 1273 and 1373 K for 1 h. From the left figure, the bimodal distribution of precipitate size (larger and smaller ones) can be seen

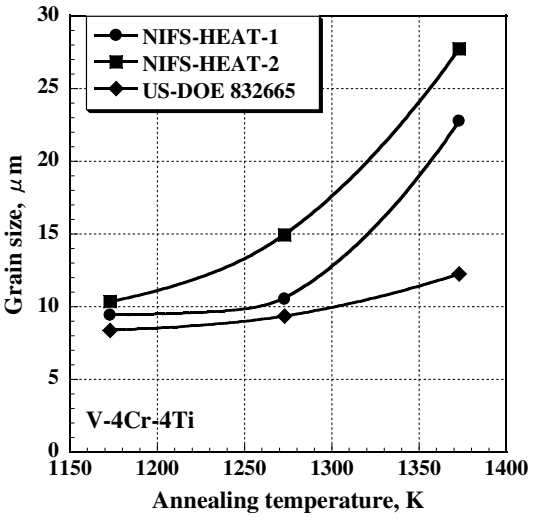

Fig. 4. Changes of grain size from 1173 to 1373 K in three alloys. The grain size increased with the decrease of the oxygen level.

in the NIFS-HEAT-1 annealed at 1273 K. However, the smaller precipitates disappeared in NIFS-HEAT-1 annealed at 1373 K. The chemical analyses of both precipitates have been done to determine the character of the precipitates. Fig. 9 shows the spectrum of TEM–EDS obtained from the matrix, large and small precipitates, as shown in Fig. 8. Fig. 9 shows that both precipitates are Ti-rich and Ti–C–O complexes, respectively. Ti-rich precipitate is mainly composed of Ti, but containing low levels of C, N, and O.

Fig. 10 shows the result of compositional analysis for the precipitates observed inside band structures using SEM–EDS. The concentration of Ti, C, N and O was observed in the bulky precipitates. Especially, among them the peak for Ti was much higher.

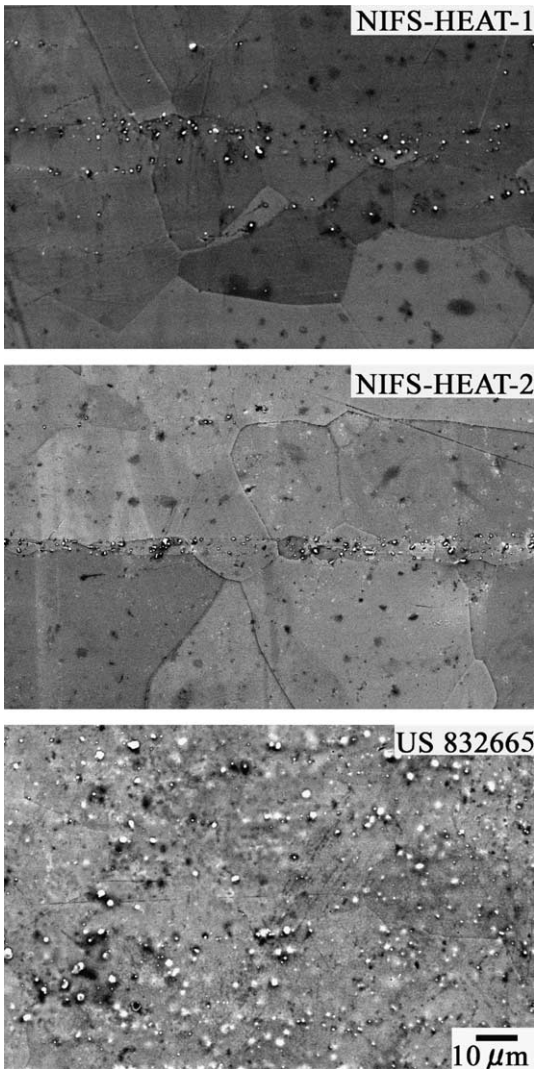

Fig. 5. Distribution of the precipitates in the transverse plane of the specimens annealed at 1273 K for 1 h. The band structure of the precipitates was observed in NIFS-HEATs. On the other hand, the precipitates were distributed uniformly in US 832665.

4. Discussions

Two kinds of precipitates were observed in all specimens annealed at 1273 K for 1 h. TEM observation reveals that the morphology of the larger and smaller precipitates was bulky and plate-like, respectively. From the TEM–EDS analyses (Fig. 9), large precipitates were identified to be Ti-rich and small were to be Ti–C–O compounds. In a previous study, the plate-like small precipitates and bulky large precipitates were observed in the NIFS-HEAT-1 and US 832665 annealed repeatedly from 973 to 1273 K after annealing at 1373 K for 1 h [14]. The small precipitates disappeared by annealing at 1373 K, but large precipitates remained in the specimens. The results of TEM–EDX observation revealed that their composition is the same as that of the precipitates observed in the previous study. From these results, it can be imagined that the smaller precipitates are stable at 973–1273 K, and dissolve into the matrix by annealing at 1373 K, leaving the bulky larger precipitates in the specimens.

Only the bulky Ti-rich precipitates are observable by SEM. SEM observation reveals that the distribution of the bulky Ti-rich precipitates was heterogeneous. The bulky Ti-rich precipitates were aligned as a band structure parallel to the rolling direction, as shown in Fig. 5. TEM–EDX and SEM–EDX analyses reveal that the large precipitates observed by TEM are the same as

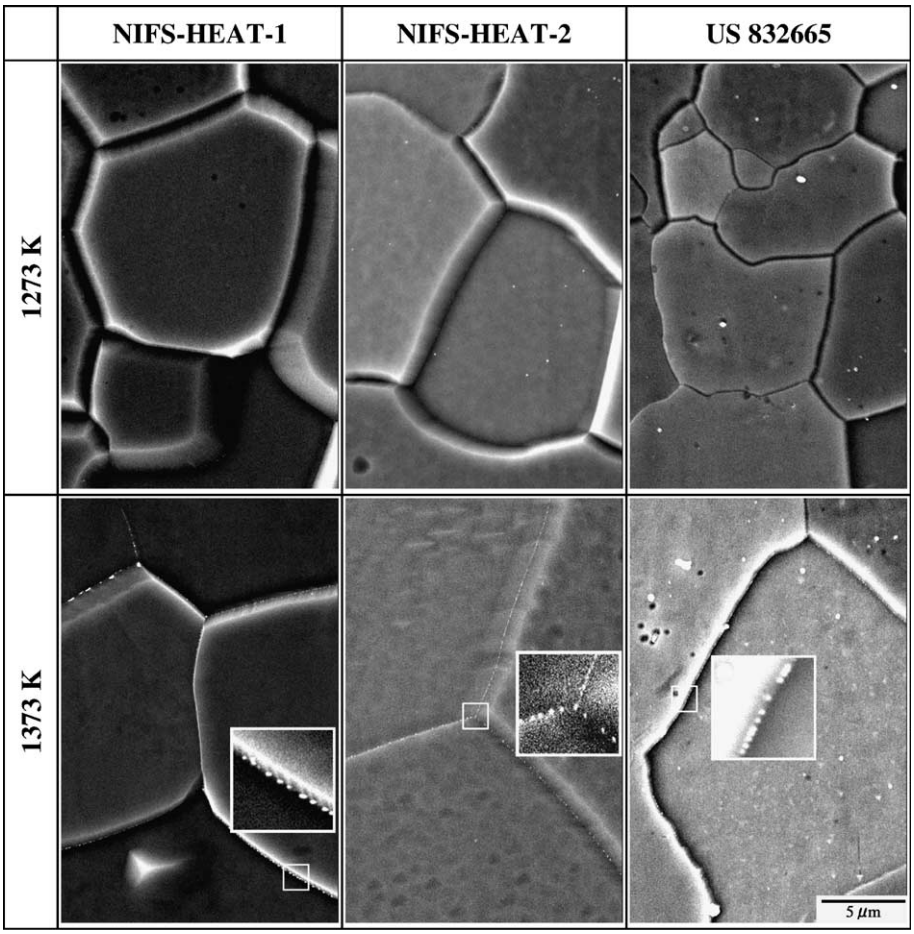

Fig. 6. SEM images of the specimens annealed at 1273 and 1373 K for 1 h. Fine precipitates were observed on the grain boundaries after annealing at 1373 K.

those observed by SEM, as shown in Figs. 9 and 10. They seem to be characterized as Ti-rich precipitates. The Ti-rich precipitates for some V–Cr–Ti alloys were observed, and their characterization was carried out. Their characterization were reported as a Ti(C, N, O) or (Ti, V)O [7,15]. But it is likely that their stoichiometry is changeable by the thermomechanical treatment.

It is likely that Ti-rich precipitates were already present after hot rolling, following melting. In the previous study, annealing of as-melted NIFS-HEAT-2 at 1423 K for an hour resulted in the formation of the Ti-rich precipitates [12]. The band structure of the precipitates in NIFS-HEATs, as shown in Fig. 5, was considered to be formed, as a result of the elongated precipitate distribution parallel to the rolling direction induced by the rolling process.

It is reported that the precipitate bands were also observed in US 832665 after hot extrusion [13]. In the

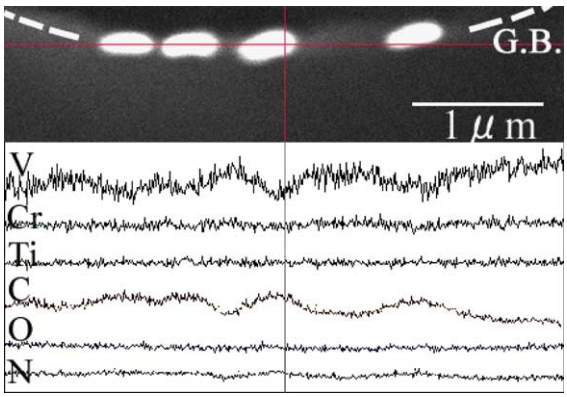

Fig. 7. A result of SEM–EDS analysis for precipitates on a grain boundary in NIFS- HEAT-1 annealed at 1373 K for 1 h. Carbon content is higher at and around the precipitates. No peak of other element was identified.

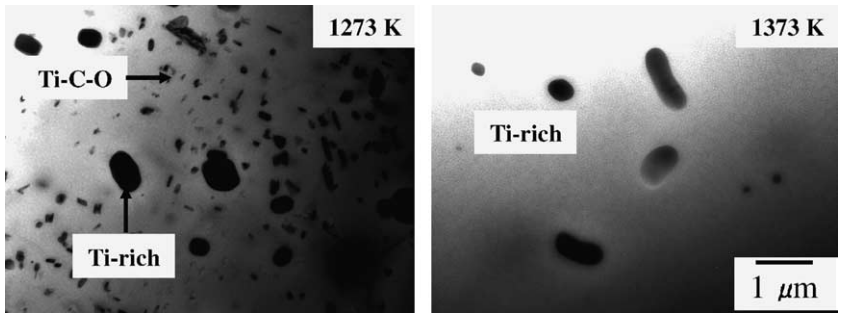

Fig. 8. TEM images of the NIFS-HEAT-1 specimens annealed at 1273 and 1373 K. Two kinds of precipitates were observed at 1273 K. Only larger precipitates were observed at 1373 K.

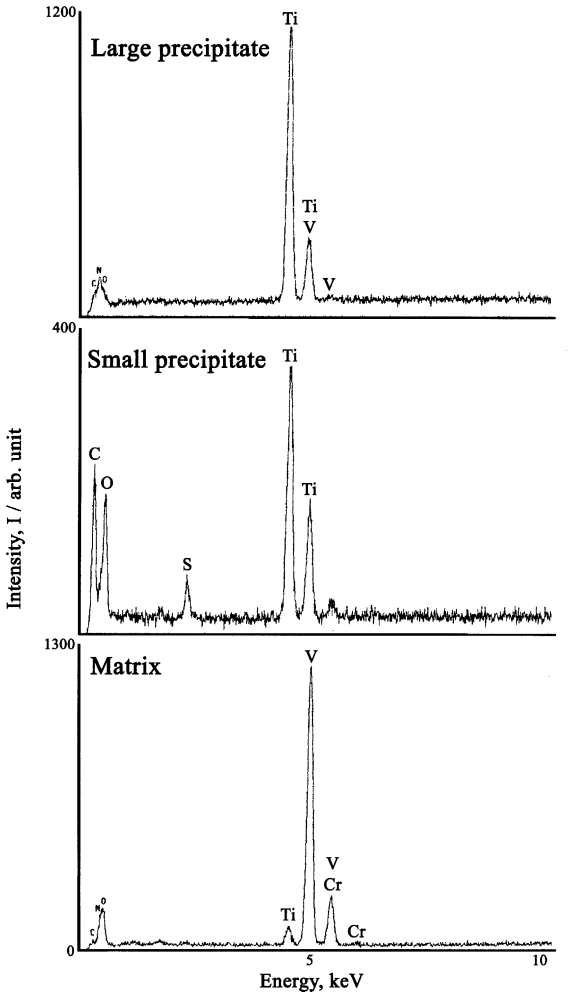

Fig. 9. A TEM–EDS analysis on the precipitates and in the matrix. The analysis reveals that large precipitates were Ti-rich, and small were Ti–C–O. The peak of sulfur is thought to be originated from residual electrolyte (H_2SO_4) used for electropolishing.

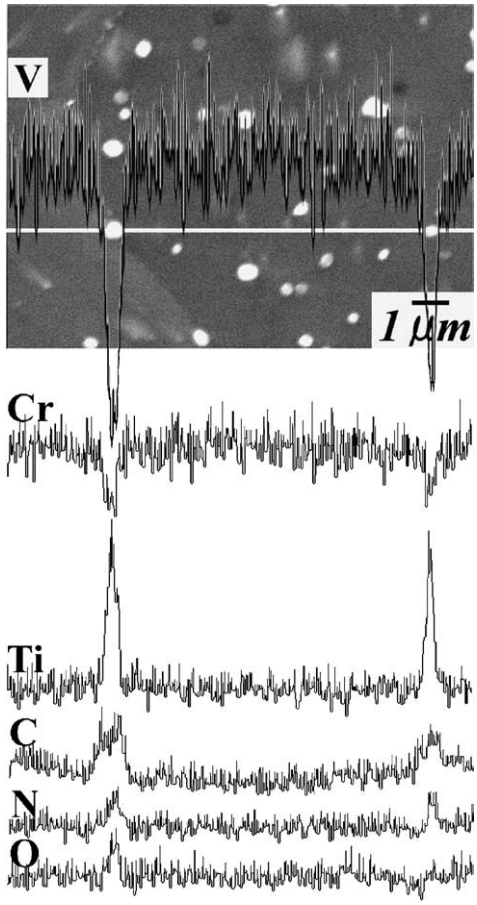

Fig. 10. A result of compositional analysis for the precipitates observed inside band structures using SEM–EDS. The concentration of Ti, C, N and O was observed in the bulky precipitates.

present study, however, the precipitates were uniformly distributed. The collapse of the band structure of the precipitates in US-DOE 832665 is likely to be due to the high degrees of rolling (>99% after hot extrusion) before annealing, relative to 90% for NIFS-HEATs. In the previous study, high thickness reduction by cold rolling (the degrees of cold rolling was about 99% after

hot working) also resulted in the collapse of the band structure in NIFS-HEAT-2 [12]. The reason of the apparent collapse may be due to the fact that the interval between bands decreases with the increase in the rolling degree and becomes comparable to the spacing between the neighboring precipitates. This means that the band structure of the Ti-rich precipitates is likely to be changed by the thermomechanical treatment or by increase in the thickness reduction.

The hardness recovery curve and initiation of recrystallization were not influenced significantly by the impurity level. From the result of the SEM observation, recrystallization already occurred at about 873 K, as shown in Fig. 2. At this temperature, hardness decrease also started in all specimens. In hardness curves shown in Fig. 1, the hardness for the NIFS-HEATs dropped significantly at 1073 K of annealing temperature. TEM observation showed that any strain introduced by rolling did not remain in recrystallized grains in NIFS-HEATs annealed at 1073 K. However, the strains introduced by rolling still remained in US 832665 annealed at 1073 K. The difference in hardness at 1073 K between NIFS-HEATs and US 832665 is thus due to the difference in the remaining strains.

The decreasing order of grain-growth rate during annealing is as follow: NIFS-HEAT-2, NIFS-HEAT-1 and US-DOE 832665. From Fig. 4, it is suggested that the distribution of Ti-rich precipitates and the impurity level influences the grain-growth rate in the recrystallization process. In particular, the grain size near the band structure of the Ti-rich precipitates was much smaller than that of grains away from the precipitates bands, as shown in Fig. 2. The grain size during the recrystallization process may be suppressed by the Ti-rich precipitates, because the secondary precipitates suppress the migration of the grain boundary. The Ti-rich precipitates are likely to be enhanced with the increase of the impurity levels [14]. Therefore, the small grain size of US-DOE 832665 may be due to the uniform distribution of the Ti-rich precipitates, which suppress the grain coarsening all over the matrix.

Another characteristic of the precipitation behavior at 1373 K is the formation of precipitates on grain boundaries (Fig. 6). As shown in Fig. 7, enrichment at the precipitates was observed for carbon, but not for chromium, titanium, oxygen or nitrogen. Therefore the precipitates formed at 1373 K on grain boundary were expected to be vanadium–carbide.

There is a tendency for hardness to increase with annealing temperature above the temperature where the hardness dropped rapidly around 1173 and 1273 K, as shown in Fig. 1. Hardening above 1273 K of annealing temperature was observed in other studies [16,17]. From SEM and TEM analysis in this temperature regime, Ti–C–O precipitates appeared at 973 K [14] and dissolved at 1373 K. Moreover, vanadium–carbide precipitates were formed on the grain boundary at 1373 K. From the microstructural evolution during the annealing treatment, the impurities are dissociated from the precipitates and distributed homogeneously in the solid solution at 1373 K. Some impurities migrate to the grain boundary to form vanadium–carbide on the grain boundary. The behavior of the impurities in V–Cr–Ti alloys during heat treatment controls the microstructure and the mechanical properties. It is thought that increase in the hardness above 1273 K is due to the increase in solid solution impurities caused by the re-solution of the Ti–C–O precipitates.

The peak of sulfur was observed occasionally in small precipitates, as shown in Fig. 9. It was reported that the precipitates are containing sulfur [15]. Thus, the peak of sulfur for the precipitates is considered as a contamination from the electrolyte, because sulfuric acid solution was used for the electrolyte in this study.

It is reported that the DBTT of V–Cr–Ti alloys increases when the annealing temperature exceeds 1273 K [18]. It is expected that the increase of the DBTT is due to the increase in the solid solution impurities and the precipitates formed on grain boundaries. The present study strongly suggests that the annealing temperature for V–4Cr–4Ti should be 1273 K or below to obtain good mechanical properties.

5. Conclusions

The behavior of hardness recovery, recrystallization and precipitation was investigated, using three kinds of V–4Cr–4Ti alloys with different oxygen contents.

(1) Irrespective of the oxygen content, behavior of hardness curve, precipitation and initiation of the recrystallization was similar to each other. Hardness decrease and recrystallization started around 873 K. In all specimens, annealing above 1273 K resulted in increase in hardness.
(2) The recrystallized grain size from 1173 to 1373 K was significantly influenced by the distribution of the Ti-rich precipitates. The rate of grain growth decreased with the increase in the impurity level, because Ti-rich precipitates are enhanced with the increase of the impurity levels.
(3) Two kinds of precipitates were observed in all specimens annealed at 1273 K. From the TEM analysis, larger precipitates were identified to be Ti-rich and smaller ones were Ti–C–O compounds. The Ti–C–O precipitates disappeared by annealing at 1373 K. Vanadium–carbide precipitates were formed on grain boundaries, as the same time. It is thought that increase of hardness above 1273 K is due to the re-solution of the Ti–C–O precipitates, and resulting increase in the solid solution level of the impurities. This is consistent with the reported DBTT shift by

increasing the annealing temperature. Based on the results, the final annealing temperature for V–4Cr–4Ti is recommended to be 1273 K or below for the purpose of obtaining good mechanical properties.

(4) The band structure of the Ti-rich precipitates was observed in NIFS-HEATs, but not in US 832665. It is considered that high degree of cold rolling after the melting contributes to the absence of the band structure in the US 832665. The band structure of precipitates influences the recrystallization behavior. It is necessary to investigate the effect of the band structure on other properties of the alloys.

References

[1] R.J. Kurtz, K. Abe, V.M. Chernov, V.A. Kazakov, G.E. Lucas, H. Matsui, T. Muroga, G.R. Odette, D.L. Smith, S.J. Zinkle, J. Nucl. Mater. 283–287 (2000) 70.
[2] S.J. Zinkle, H. Matsui, D.L. Smith, A.F. Rowcliffe, E. van Osch, K. Abe, V.A. Kazakov, J. Nucl. Mater. 258–263 (1998) 205.
[3] H. Matsui, K. Fukumoto, D.L. Smith, H.M. Chung, W. van Witzenburg, J. Nucl. Mater. 233–237 (1996) 92.
[4] B.A. Loomis, H.M. Chung, L.J. Nowicki, D.L. Smith, J. Nucl. Mater. 212–215 (1994) 799.
[5] T. Muroga, T. Nagasaka, A. Kawabata, S. Sakurai, M. Sakata, J. Nucl. Mater. 283–287 (2000) 711.
[6] T. Nagasaka, T. Muroga, M. Imamura, S. Tomiyama, M. Sakata, Fus. Technol. 39 (2001) 659.
[7] H.M. Chung, B.A. Loomis, D.L. Smith, J. Nucl. Mater. 239 (1996) 139.
[8] W.R. Johnson, J.P. Smith, J. Nucl. Mater. 258–263 (1998) 1425.
[9] D.R. Diercks, B.A. Loomis, J. Nucl. Mater. 141–143 (1986) 1117.
[10] H.M. Chung, B.A. Loomis, D.L. Smith, J. Nucl. Mater. 239 (1996) 139.
[11] M.L. Grossbeck, J.F. King, D.J. Alexander, P.M. Rice, G.M. Goodwin, J. Nucl. Mater. 258–263 (1998) 1369.
[12] T. Nagasaka, N.J. Heo, T. Muroga, M. Imamura, Fus. Eng. Des. 61&62 (2002) 757.
[13] Y. Yan, H. Tsai, D.L. Smith, Fusion Materials Semiannual Progress Report for period ending 31 December 1999, DOE/ER-0313/27, 1999, p. 23.
[14] N.J. Heo, T. Nagasaka, T. Muroga, H. Matsui, J. Nucl. Mater. 307–311 (2002) 620.
[15] D.S. Gelles, P.M. Rice, S.J. Zinkle, H.M. Chung, J. Nucl. Mater. 258–263 (1998) 1380.
[16] A.N. Gubbi, A.F. Rowcliffe, J. Nucl. Mater. 233–237 (1996) 497.
[17] D.T. Hoelzer, M.K. West, S.J. Zinkle, A.F. Rowcliffe, J. Nucl. Mater. 283–287 (2000) 616.
[18] K. Fukumoto, T. Morimura, T. Tanaka, A. Kimura, K. Abe, H. Takahashi, H. Matsui, J. Nucl. Mater. 239 (1996) 170.